DFG-reference number: GA 1704/1-1

Authors: A. Soleimani Dorcheh, Mathias C. Galetz

Institute/department : DECHEMA-Forschungsinstitut/ High Temperature Materials

Topic of the project: The High-Temperature Stability of Cr-Si-Ge alloys

Period covered by the report, overall funding period: 01.03.2012-30.09.2014

List of the most important publications resulting from this project.

A. Soleimani-Dorcheh, M.C. Galetz, *Oxidation and Nitridation Behavior of Cr–Si Alloys in Air at 1473 K*,Oxidation of Metals, 2015

A. Soleimani-Dorcheh, W. Donner, M. C. Galetz, *On ultra-high temperature oxidation of Cr–Cr3Si alloys: Effect of germanium,* Materials and Corrosion 65 (12), 2014, 1143

A. Soleimani-Dorcheh, M.C. Galetz, *Cr-Ge-Si Alloys for High-Temperature Structural Applications: Microstructural Evolution*, Metallurgical and Materials Transactions A 45 (3), 2014, 1639

1. Introduction

Increasing efficiency, reducing CO_2 emission and fuel consumption are of the most important challenges in high temperature technologies. Higher efficiencies can be achieved by increasing the operating conditions (temperature and pressure). This has challenged materials science community to improve high temperature properties of the existing materials or pursue novel materials for higher temperatures. For more than 60 years this goal was achieved by enhancing the high temperature properties of Ni-base superalloys. Modification of the composition with more than 10 micro-macro alloying elements and engineering of the microstructure with γ -γ' phase system has significantly increased its mechanical properties and environmental resistance till up to 1150°C. However, due to the softening of Ni above 1150°C there is no more scope to increase the service temperature of such alloys[1, 2] and demands raised for new materials replacing Ni-base superalloys.

Structural intermetallics (such as $MoSi_2$, Nb_5Si_3, and Cr_3Si) and their alloys have recently attracted attentions since these materials overcome the melting point and possess high temperature mechanical strength.

The most studied system is Mo and its alloys especially in Mo-Si-B system which offers high temperature strength at temperatures beyond Ni base superalloys. However, it suffers the formation of metastable phases and pesting at moderate temperatures (600°C) and week oxidation resistance at high temperatures (> 1000°C)[3].Alternatively, niobium and its alloys, especially in Nb-Nb_5Si_3 system are studied. Nb and its alloys offer ultra-high melting point > 1800°C, low density and high temperature strength. Nevertheless, it suffers the rapid oxidation scaling and embrittlement by oxygen dissolution at ultra-high temperatures.[4-6]

Chromium and its alloys are considered as potential candidate for high temperature applications because of its high melting point (1900°C), low density (7.15 g/cm3) (Ni=8.90 g/cm3) and high-temperature oxidation resistance and high abundance in the earth crust. These advantages are negated by low ductility at room temperatures (a typical feature in all BCC metals), Nitrogen embrittlement in air at high temperature due to severe nitridation and low oxidation resistance at ultra-high temperatures (>1000°C) due to the volatilization[7-9]. Researchers have been working on enhancing the mechanical and high temperature performance of Cr-based alloys by micro-macro alloying with binary-ternary or quaternary elements such as Al, Ag, Si, Mo, Ta, W, Ru, Ce, and Nb [4, 10-18]. As a result of alloying, some of these drawbacks are improved [18-20]. Some of the alloying elements form a two phase system with chromium composed of a toughening Cr solid solution phase along with an intermetallic hardening phase which is formed via solidification and thus are called in-situ composites. Cr_{ss}-Cr_2X alloys (X= Nb, Hf,Ta, Zr) form a eutectic microstructure containing laves phase Cr_2X particles or lamellae dispersed in a solid solution phase (Cr_{ss}).

1.1 Cr-Cr_3Si System

Cr_{ss}-Cr_3Si system forms a lamellar eutectic structure consisting of Cr_{ss} and Cr_3Si A15 phase [4]. In this system, the A15 intermetallic phase is a source of high temperature strength and oxidation resistance and Cr_{ss} is a potential source of ductility[4, 21, 22]. There are only limited numbers of studies on the high temperature behavior of single phase Cr_3Si and the Cr_{ss}-Cr_3Si system [23, 24].

1.2 Effect of Germanium alloying

Synergic effects of Ge and Si attracted interests in developments of high temperature alloys and protective coatings [6, 25-27]. Germanium doping in silicide coatings on refractory metal substrates showed a significant improvement in their high temperature oxidation [6]. Similarly, Ge alloying of Nb-Silicide system showed significant improvements in high temperature oxidation [28, 29]. The high temperature oxidation resistance of Ge-alloyed system is due to the formation of a SiO_2-GeO_2 protective layer.

In this work, high temperature oxidation behavior of the Cr-Si system is studied. The effect of Si on high temperature oxidation/nitridation of chromium is explored. Effect of Ge-alloying on microstructure, phase diagram, and high temperature stability of Cr-Cr_3Si system is studied. Phase analysis, phase diagram assessment, microstructural evolution and oxidation-nitridation properties of alloys in high chromium end of Cr-Ge-Si ternary system were investigated and compared to the reference binary Cr-Cr_3Si system.

1.3 Project scopes:

The use of Ge as alloying element for high temperature alloys was promising. Cr-Cr_3Si system has shown high temperature mechanical and microstructutral stability and using Ge as substituting element for Si was an idea to tune the microstructure for higher stability at high temperatures. It was aimed to explore the ternary Cr-Si-Ge system and evaluate the effect of Ge on microstructural evolution and oxidation behavior of the binary Cr-Si system at high temperatures (above 1150°C). More specifically, the effect of Ge-Si substitution on:

a. Oxide growth kinetics
b. Stability of oxide in cyclic exposures
c. Oxide scale adherence
d. Phase transformation and stability of microstructure (coarsening) at high temperature
e. Crystallographic study of the intermetallic A15 phase and solid solution phase
f. Characterization of the ternary phase diagram at high chromium end

1.4 Project Development:

The initial scopes of the project were mostly met during the project. The project started with a background research via characterization of the novel Cr-Ge-Si system and understanding the oxidation behavior of the Cr-Si system. The ternary phase diagram, microstructural evolution and phase transformation at the Cr-rich corner is studied. The high temperature oxidation behavior of the Cr-Si system in multi-oxidant atmosphere (air) was systematically studied and the behavior of single phase Cr-solid solution and intermetallic A15 silicide were characterized. At this stage, the focus was not only on the oxidation, but also on the nitridation behavior of the substrate alloy during the exposure. It developed to the optimization of the system against oxidation-nitridation at high temperatures. At the last stage it was tried to understand the mechanisms behind the behavior of the optimized system and to move towards a possible up scaling for industrial applications. The microstructural coarsening is qualitatively evaluated when the microstructural evolution were studied. However, efforts to quantify the microstructural coarsening and the effect of Ge on the coarsening rate could not be conducted due to the technical issues. The nitridation of Cr_{ss} phase in alloys microstructure when annealed at high temperatures in Ar-5%H_2 atmosphere did not allow a successful modeling.

2. Experimental

2.1 Casting and sample preparation

Three batches of binary and ternary alloys have been prepared in Cr-rich part of the Cr-Si and Cr-Si-Ge systems. Alloys with were prepared as small buttons (ø=5-7 mm, m=7g) by melting high purity Cr (99.995 wt. %), Si (99.999 wt.%), and Ge (99.99 wt. %) using a compact arc melter (MAM-1, Edmund Bühler, Germany) under a high purity argon atmosphere on a water-cooled copper crucible. Before melting each ingot, a zirconium getter was melted in order to eliminate the oxygen remnants and nitrogen impurities in argon atmosphere. The buttons were turned and re-melted at least seven times to avoid macro segregation in the as cast specimens. The ingots were cut to several pieces using electric discharge machining (EDM). Since the solidification rate is different at different parts of arc melted ingots, the specimens taken for this study were all taken from the center of ingots in order to avoid comparing zones with different solidification rates.

2.2 Exposures

Oxidation experiments were performed in short term (isothermal) and long term (quasi-isothermal) exposures in synthetic air at 1473K and 1623K. Specimens used for oxidation experiments were ground (600 grit SiC paper), weighed, and degreased in acetone in an ultrasonic cleaner before being introduced to the furnace chamber.

The thermogravimetric measurements were conducted using a microbalance (Sartorius Micro M25-D-V, Germany) which was equipped with a vertical tube furnace. The alloy coupon was attached to the balance with a platinum wire and held inside the hot zone of the furnace. While the balance was stabilized at room temperature, synthetic air was introduced to the furnace chamber at a linear flow rate of 203 cmh^{-1}. A heating ramp of 20 K/min was applied to reach the test temperature at 1473K. Isothermal exposure was conducted for 100h and finally the sample was cooled down to room temperature in the furnace. A reference measurement was performed with the same test parameters in order to exclude instrumental artifacts such as Pt evaporation. The reference profile was subtracted from the specimen's mass gain profile. The TG-measurement was repeated for a random specimen to verify the reproducibility of the test [30]. Long-term quasi-isothermal oxidation tests were conducted at 1473K in a tube furnace connected to a synthetic air atmosphere with a 203 cmh-1 linear flow rate. The samples were placed separately in alumina crucibles and removed from the furnace after 500 and 1000 hours of cumulative exposure for 1473K and 1623K, respectively. Oxidized specimens were coated with Ni via electroplating to protect oxidation products (oxide remnants) during preparation and to provide enhanced contrast during imaging.

For microstructural analysis, the as cast specimens were annealed at 1473K for 100 hours in a tube furnace under Ar-5%H_2 flow using titanium powder as oxygen getter. For crystallographic characterization alloys were annealed in Ar-5%H_2 atmosphere at 1623K for 100h. After heat treatment alloys were cooled down to room temperature in the furnace. Prior to metallographic study and elemental analysis, cross sections were wet ground down to 1200 grit SiC paper followed by a final polishing step using 3µm and 1µm diamond and 0.02 µm SiO_2 pastes.

2.3 Characterization

The actual composition of the studied alloys was obtained by Wavelength Dispersive Spectrometry (WDS). Multipoint grid (10×10) quantitative measurements were performed at three different zones in each specimen using a JEOL JXA-8100 electron probe micro analyzer (EPMA). Microstructures were characterized by SEM and EPMA using Fe_4N and Al_2O_3 standards for nitrogen and oxygen, respectively. Pure Si and Cr were used as standards for quantitative measurement of the alloys.

A Brucker D8 advance diffractometer with Cu-Kα radiation was used for phase analysis of alloys. Phase identification was performed by comparison of the diffraction patterns to the International Centre for Diffraction Data's Powder Diffraction File (PDF).

The indentation hardness of alloys was measured using a Nano-indentation tester (NHT^2, CSM Instruments-Switzerland) with a Berkovich tip. Displacements (h) and loads (P) were recorded at 295K with a maximum load of 15 mN and constant loading and unloading rate of $\dot{P}/P = 0.06\ S^{-1}$.

3. Results

3.1 Oxidation/Nitridation in Cr-Si system

This part is recently published in Oxidation of Metals, 2015. Please see the attachments.

The evolution of Cr-Si alloys with different microstructures during high temperature oxidation is investigated. The effect of Si content and as-cast microstructure is correlated to the oxidation and nitridation behavior. Particular attention is paid to the evolution of nitride phases in the subscale region during oxidation. The following conclusions were made at the end of this part:

1. Addition of Si significantly improved the oxidation resistance of chromium and slowed down the formation of subscale Cr_2N in the substrate.
2. Single phase A15 Cr_3Si showed high temperature stability and almost complete nitridation resistance even up to 1000 hours exposure at 1473K. In A15 the microstructural evolution below the oxide scale can be directly related to the significantly higher diffusion rate of Cr in Cr_3Si than Si, so Cr builds up the oxide scale and Cr-depleted Cr_5Si_3 is initially formed at the metal-oxide interface during oxidation. On the other hand, Si is the faster species in Cr_5Si_3 which promotes selective Si diffusion towards the surface and facilitates the formation of SiO_2 scale which consequently improves the oxidation kinetics.
3. In Cr-Cr_3Si eutectic alloys, the chromium solid solution phase was selectively oxidized and stabilized the A15 silicide layer below the oxide scale. This layer acted as a barrier to the inward diffusion of nitrogen which protects the substrate against nitridation. In the absence of the A15 subscale layer, selective nitridation of the solid solution phase resulted in the formation of an interconnected nitride network.

3.2 Germanium alloying of Cr-Cr_3Si

3.2.1 Microstructural Evolution

This Part is published in Metallurgical and Materials Transaction A, 2014. Please see the attachments.

The microstructural evolution of the Cr-Ge-Si system upon variation of the Si/Ge ratio was studied. The Cr-rich part of the ternary diagram is experimentally developed and the phases were characterized by phases and elemental analysis methods. The mechanical properties of each phase were accordingly studied using indentation methods.

The followings were concluded from the results:
1- All alloys with a composition in the range of Cr-Si_{15-x}-Ge_x (0<x<15) are located in a two phase field of the ternary diagram consisting of Cr_{ss} and Cr_3(Si, Ge) A15, so that Ge and Si can substitute each other in a full composition range.
2- No intermediate phases were observed in the studied composition range.
3- Increasing Ge/Si ratio significantly changed the microstructure from a fine lamellar network towards a coarser microstructure composed of primary chromium phase embedded in an A15 matrix. At Ge/Si>25%, the microstructure directly reflects the transition from the eutectic to the peritectic transformation.
4- The solubility of Cr_{ss} in binary alloys (Cr-Ge and Cr-Si) is higher than that in Cr-Ge-Si ternary alloys. However, due to the coarser Cr_{ss} phase in ternary systems, A15 precipitates within the solid solution phase after an annealing process are significantly more than in binary alloys.
5-Indentation hardness results prove that in all alloys, Cr_{ss} acts as the toughening phase with significantly higher deformability at the same loading condition at room temperature than the intermetallic A15 phase.

3.2.2 Germanium effect on lattice parameter of Cr_{ss} and A15 Silicide phase

The lattice parameters of the two phase Cr-Cr_3Si system were determined using X-ray diffraction method. All alloys with compositions in the range of $Cr85Si_{(15-X)}Ge_X$ where 0<x<15 were characterized and the lattice parameters were obtained using Nelson-Riley extrapolation method [31]. Lattice parameters of the Cr_{ss} and A15 silicide phase are illustrated in Fig. 1. It shows that replacing Si with Ge linearly increases the lattice parameter of both bcc solid solution and A15 intermetallic structure

(according to Vegard's law). It is not surprising when the atomic size of Si (117.6 pm) and Ge (125 pm) are considered. A linear fit is used to quantify the effect of Ge on each crystal structure. The effect of Ge on the lattice parameter of the A15 phase is significantly (by a factor of 2.7) higher than the solid solution phase. The lattice misfit (δ) between Crss and A15 phase in each Ge/Si ratio is illustrated in Fig. 2 using equation (1).

$$\delta = \frac{2(a_{[Crss]} - a_{[A15]})}{(a_{[Crss]} + a_{[A15]})} \quad (1)$$

The lattice misfit of 45-46% indicates that approximately every two continuous planes in the A15 phase will take a dislocation to accommodate the misfit of the two lattices which categorized their interface as "incoherent interface".

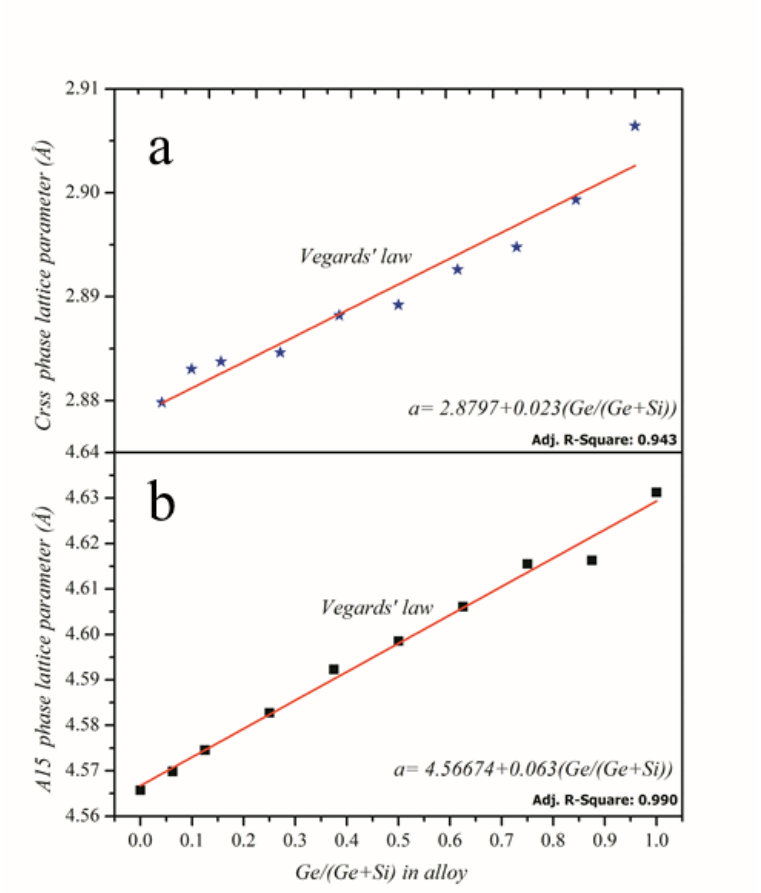

Fig. 1 The effect of Ge-Si substitution on the lattice parameter of a) Cr-solid solution and b) A15 intermetallic phase in two-phase Cr-Si-Ge alloys. The linear fit shows the Vegard's law for solid solution effect on lattice parameter.

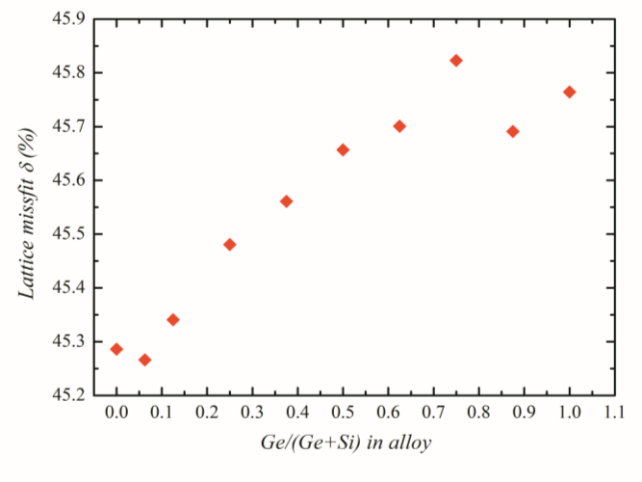

Fig. 2 The lattice misfit between the A15 intermetallic phase and Cr-solid solution phase upon Ge-Si substitution in Cr-Si-Ge alloys

3.2.3 Germanium effect on high temperature oxidation of the Cr-Cr_3Si system

This part is published in Materials and Corrosion, 2014.

The oxidation kinetics of Cr-Cr_3 (Si, Ge) alloys within the composition range of $Cr_{85}Ge_XSi_{15-X}$ (0<x<15) at ultra-high temperatures (1623K) were studied. The oxide scales formed during the isothermal oxidation were characterized and the followings could be concluded from the results.

1. Two mechanisms of parabolic growth and linear evaporation are simultaneously involved in ultra-high temperature oxidation kinetics of Cr-Si-Ge alloys.

2. Addition of up to 2 at% Ge significantly reduced the volatilization and oxidation rates, while in the alloy with high Ge content (12%) these parameters increased.

3. The predominantly oxide on the gas–scale interface is chromia.

4. Silica shows a finely dispersed crystalline morphology at oxide–substrate interface in binary Cr–Si alloy while low Ge-alloyed sample results in the formation of a thin SiO_2 crystalline layer, which partially covered the surface. The silica layer was in charge of the improved oxidation kinetics of alloys with up to 2 at% Ge.

5. After 100 h of oxidation at 1623K, the protective scale consists of fine-grained chromia with embedded large hexagonal single crystals.

3.2.4 Ge effect on nitridation behavior of Cr-Cr_3Si alloys

Nitridation is the most challenging obstacle to the high temperature application of chromium and its alloys. Thus, it is necessary to put emphasis on nitridation of chromium alloys when studying oxidation in nitrogen containing atmospheres (e.g. air). The nature of chromium nitride, its stability and its evolution during the oxidation of Cr-Si alloys were extensively discussed in our publication [32]. As mentioned in chapters 3.1, in contrast to the solid solution chromium, Cr_3Si is stable at all nitrogen partial pressures and does not nitride when exposed to air at high temperatures [32]. Additionally, it is known that the diffusion of interstitial elements i.e. O and N is limited in A15 structures [33]. In Cr-Cr_3Si alloy, dissolution and selective oxidation of the Cr-solid solution phase forms an A15 Cr_3Si layer at the subscale zone which protects the substrate alloy from selective nitridation of the solid solution lamellae [32]. Cr is still the dominant diffusive element in the A15 structure [34, 35], however. Thus, as a result

of the massive diffusion of Cr through the A15 layer, Kirkindal pores form within the A15 layer which can facilitate the access of nitrogen to the substrate microstructure. At this stage, the A15 layer does not act protective anymore (at higher exposure times) and internal nitridation of the Cr-solid solution lamellae is expected. A network of nitrided phase will form if the solid solution phase has network morphology (e.g. the eutectic microstructure).

To avoid such damage at high temperatures two strategies can be used: a. improving the stability of the A15 layer at subscale zone 2. Designing a desired microstructure consisting disconnected chromium solid solution phase isolated in the A15 network.

The mutual solubility of Si and Ge in the A15 phase and the fact that Ge promotes the formation of A15 phase were discussed in chapter 3.2.2. In this part, the oxidation kinetics and the post exposure microstructural characterization of the eutectic Cr-Cr_3Si and hyper-eutectic (with primary Cr_3Si dendrites) in binary and quasi-binary (Ge-alloyed (Ge=0-2 at%) were compared after oxidation at 1473K in synthetic air for 50 and 1000 hours. The composition of alloys is listed in Table 1. The experimental procedure was followed as explained in chapter 2. The isothermal oxidation test was carried out at 1473K for 50h using a Netzsch STA 449 F1 analyzer.

Table 1. The actual composition of alloy substrates

Alloy	Cr	Si	Ge
Cr-16Si (S16)	84.1±0.3	15.8±0.3	0
Cr-15Si-1Ge (SG1)	83.8±0.4	15.3±0.4	0.96±0.0
Cr-14Si-2Ge (SG2)	83.1±0.1	14.5±0.1	2.34±0.1

Fig. 3 illustrates the thermogravimetric results during 50h exposure. The mass change curves were fitted accordingly using the Equation 2 which evaluates the oxidation kinetics based on oxide parabolic growth and linear vaporization.

$$\left(\frac{\Delta m}{A}\right) = (k_p t)^{0.5} - k_v t \qquad (2)$$

where $\Delta m/A$ is the weight change per unit area, k_p the parabolic rate constant, k_v the volatilization rate during the time of exposure *t.* The detailed descriptions about the origin of Equation 2 and its considerations are explained in our publication [32]. As Fig. 3 shows, the alloy with 2 at% Ge shows the slowest oxidation kinetics (as it was observed at higher temperatures [30]).

Fig. 4 shows the post exposure microstructure of alloys Cr-16Si and Cr-14Si-2Ge after 50h and 1000h exposure at 1473K. The binary Cr-Cr_3Si alloy forms the A15 silicide layer at subscale interface after 50 hours of exposure. This layer is formed by dissolution of the Cr solid solution phase and transportation of chromium through the A15 phase towards the oxide-substrate interface. A thin area of selectively nitrided Cr solid solution zone is detected below the A15 layer (≈10-15µm). At 1000 hours, the A15 layer in Cr-16Si alloy is thickened (~110µm) via the further dissolution of chromium solid solution. Prominent transportation of chromium resulted in severe Kirkindal pore formation which can provide an easier access of nitrogen to the sub-layer microstructure. It should be noted that after 1000 hours exposure, the alloy substrate still shows a fine microstructure with a lamellar structure of Crss and A15 phase which is desired for mechanical aspects [2].

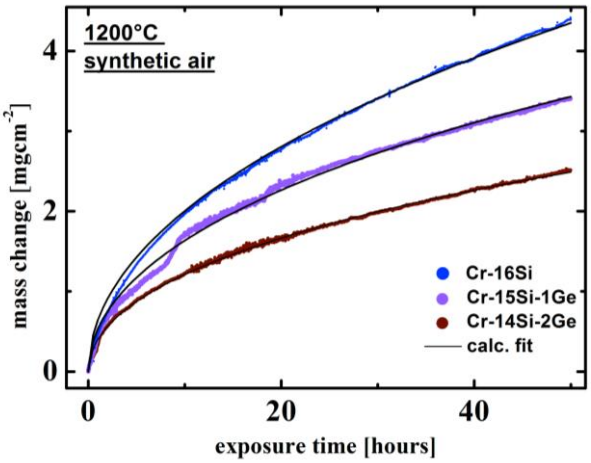

Fig. 3 The isothermal oxidation behavior of binary Cr-Cr_3Si and ternary Cr-Cr_3(Si, Ge) alloys in synthetic air at 1473K.

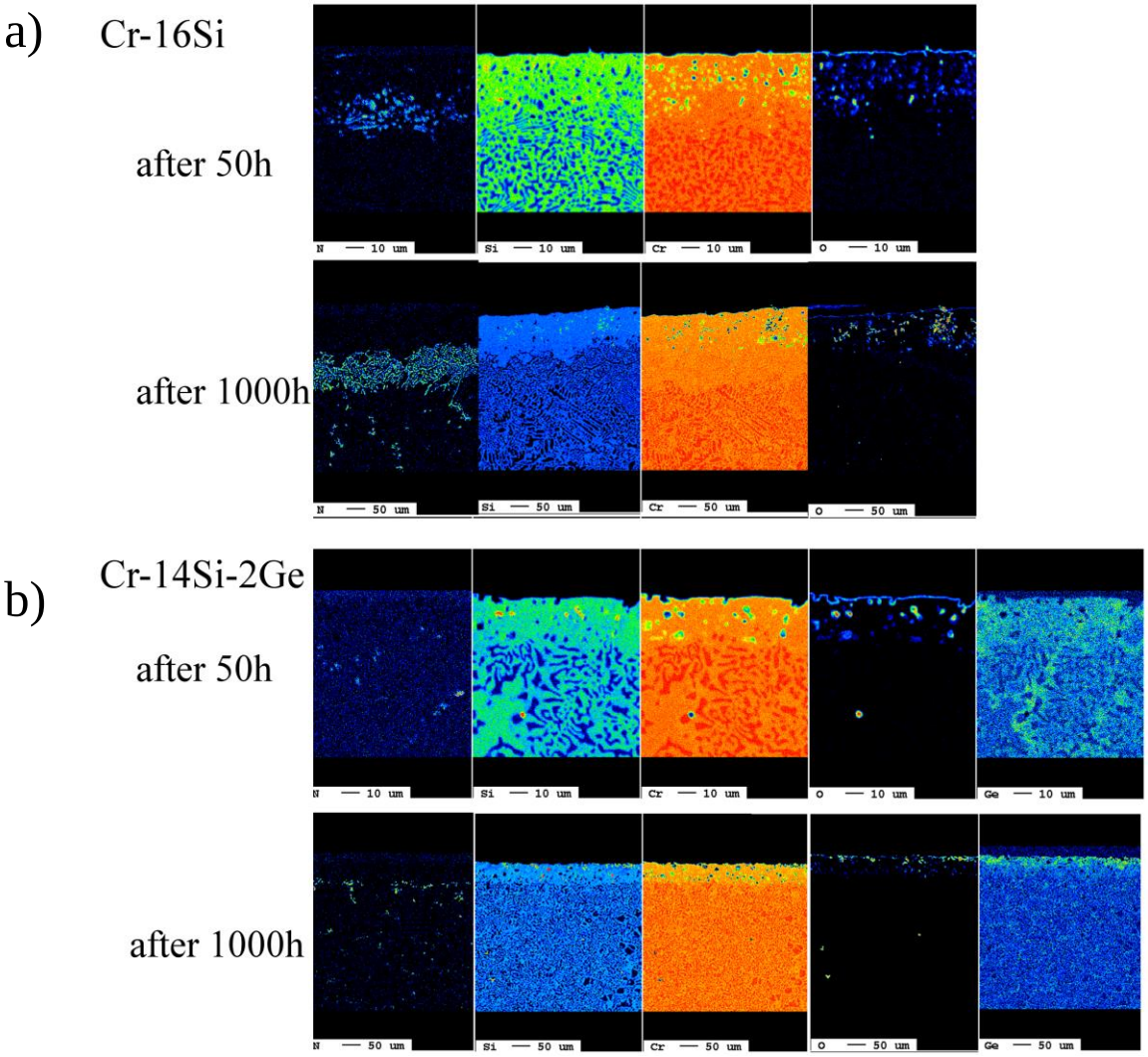

Fig. 4 Cross sectional elemental distribution maps of a) Cr-Cr_3Si and b) Cr-Cr_3(Si,Ge) after 50h and 1000h exposures at1473K in synthetic air.

The interconnected network of the Cr_{ss} lamellae when exposed to nitrogen, form a network of nitride beneath the A15 layer (Fig. 4.a) while the silicide lamellae remain protected. Fig 5.a shows the quantitative line scan starting from the oxide-substrate interface up to the end of A15 subscale layer in Cr-16Si alloy. Within the thickness of the A15 subscale layer, a slight depletion of chromium is observed while the Cr concentration is 75.4 and 77.7 at% at oxide-substrate interface and the inner end of the layer, respectively. The depletion of Si in the subscale A15 layer is not significant as the Si concentration at the two ends of layer is 22.2 and 23.9 at%.

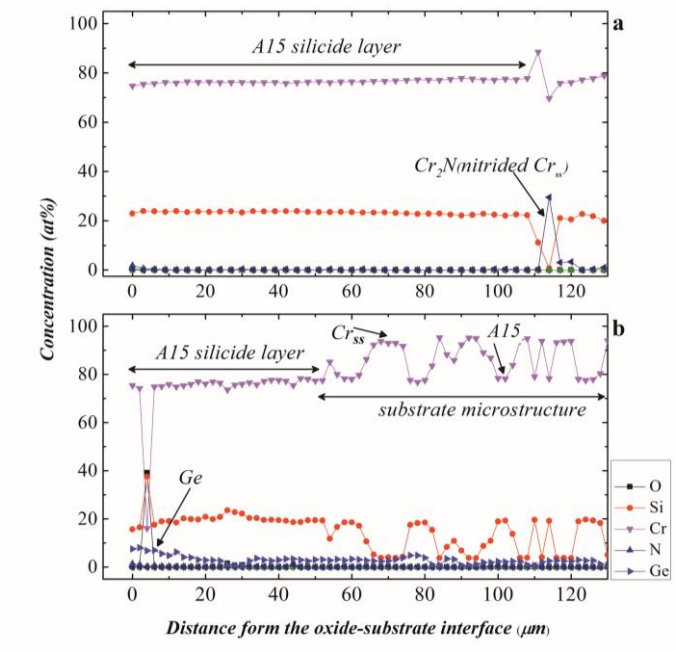

Fig. 5. The cross sectional line scan of the A15 subscale layer formed in alloy a) S16 and b) SG2 after 1000h exposure in synthetic air at 1473K.

The post exposure microstructure of alloy SG2 consists of a fine microstructure with an A15 layer at metal-scale interface. Beneath the A15 layer a fine two phase microstructure of Cr-Cr_3Si(Ge) is observed. Addition of Ge altered the microstructure towards a network of A15 silicide surrounding a fine nodular Cr_{ss} structure. It has to be noted that after 50h, Kirkindal porosities are formed at the subscale A15 layer and a negligible amount of nitrides are formed beneath the layer.

After 1000h exposure, the A15 subscale layer is grown inward while the porosities are increased. A saturation of Ge can be observed in the A15 layer at the substrate-scale interface (see Fig 4.b). Quantitative line scans in Fig. 5.b shows a thickness of ~52 µm which is significantly less than that of alloy S16 (~110µm) at similar conditions. Beneath the A15 layer no more sign of nitridation is observed. The average compositions of subscale A15 layers in both alloys are listed in Table 2. As table shows a negligible solubility of nitrogen in A15 phase can be detected while no oxygen solubility is observed.

The key question is how the ternary addition of Ge affects the oxidation and nitridation mechanism of the two phase Cr-Cr_3Si system and if Ge influences on oxidation are correlated to the nitridation process. It was shown in our study that the main oxidation product of this alloy system is chromia [30].

Table 2. The average composition of A15 silicide layer formed at scale-alloy interface after 1000h oxidation at 1473K in air

Elements	A15 subscale layer	
	S16	***SG2***
O	0	0
Si	19.7	23.3
Cr	76.4	76.6
N	0.1	0.1
Ge	3.6	N.A.

This is in agreement with subscale microstructural observations (Fig. 4 and Fig. 5). The significant dissolution of the chromium solid solution phase in subscale zone and negligible chromium depletion at the A15 Cr_3Si layer imply that the Cr-rich phase is the major chromium supply. Thermodynamics calculations of the activity of Cr, Si and Ge in binary Cr-Si and Cr-Ge system reveals a significant difference of activity of Cr (a_{Cr}) between the solid solution Cr and the intermetallic Cr_3Si phase (see Fig. 6) which shows the prominent driving force for selective oxidation of the solid solution phase. In Cr-Ge system, however, the difference between a_{Cr} of Cr_{ss} and A15 Cr_3Ge is notably decreased i.e the driving force for the selective oxidation of solid solution phase during oxidation is significantly decreased. Thus, it is not surprising to expect higher contribution of the A15 phase in oxidation process when Ge is added. This can be validated by observation of more Kirkindal porosities (as a result of local Cr outward diffusion) and higher Cr-depletion in the subscale A15 layer of alloy SG2 despite its lower thickness (see Fig. 4b and Fig. 5b). Accordingly, as the contribution of the A15 in oxidation of Ge-alloyed system is increased, the oxidation resistance enhances when Ge is alloyed (see the thermogravimetric results in Fig. 3).

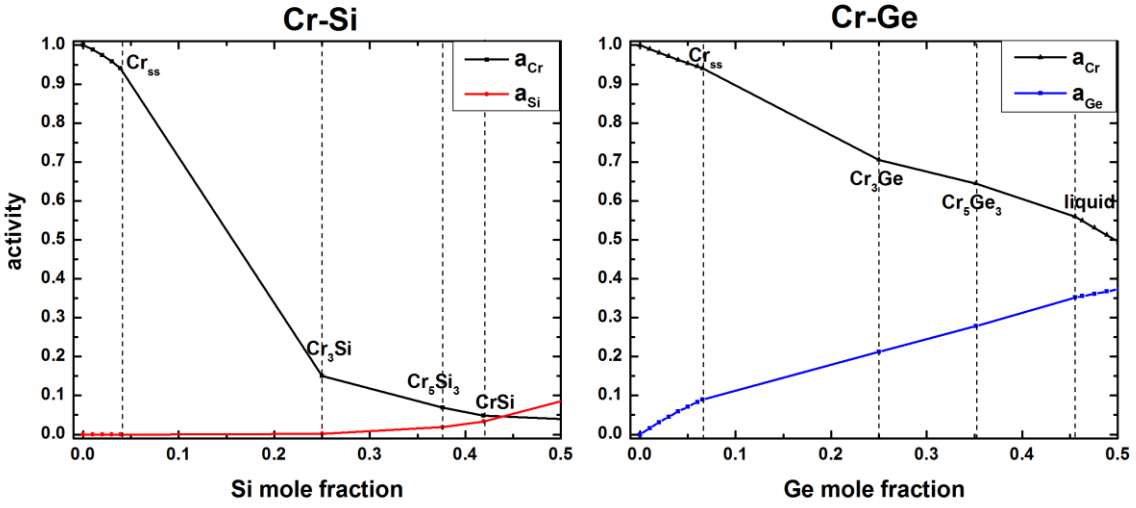

Fig. 6 Thermodynamic activity of elements in Cr-Si and Cr-Ge binary systems. Note the abrupt decrease of the activity of chromium in Cr-Si system (calculated by FactSage 6.1).

The mechanism of nitridation in binary Cr-Cr_3Si system is extensively discussed in our recent publication [32]. As illustrated in Fig. 4, germanium alloying alters the microstructure towards a semi-eutectic microstructure with network of A15 phase and isolated Cr_{ss} nodules i.e. the access of nitrogen to the solid solution phase will be suppressed by the A15 network (see Fig 4.b). This is the key influence of

Ge-addition on nitridation resistance of the Cr-Cr_3Si system. It should be noted that the amount of added Ge is significantly important since higher Ge-additions (>2 at%) introduces more primary chromium solid solution with dendritic form which coarsen the microstructure and increase the risk of nitridation [36].

4. Outlook

The Cr-Si-Ge system showed a high capability for oxidation resistance at ultra-high temperatures. In this work, it was shown that with microstructural design using Ge alloying, the nitridation of Cr at high temperatures can be significantly suppressed. As nitridation was the biggest challenge for chromium alloy development, we are encouraged to develop the studied alloy system further to improve the mechanical properties of alloys at a temperature range. Therefore a proposal for continuing the project by focusing on mechanical properties is prepared to submit to the DFG. The main idea is to design a developed alloy system with more alloying elements to toughen the chromium solid solution phase and to use the high alloying capability of chromium at high temperatures in order to precipitate the intermetallics phase via a corresponding heat treatment.

4.1 Up-scaling towards industrial applications

The results of this work attracted the interest of industries to scale up the optimized alloys via powder metallurgy. This would allow us to compare different alloy making methods and characterize the mechanical properties of alloys such as elastic modulus (E) and creep resistance.

Collaborations

The experimental results provided in this work are performed at the High Temperature Materials group of the DECHEMA-Forschungsinstitut. A part of X-ray diffraction experiments in this study was conducted in the Faculty of Materials Science, Department of Structure Research in Technical University of Darmstadt.

Qualification of Young Researchers:

This research was conducted in the framework of a PhD thesis which is in finalization stage to submit to the RWTH Aachen University (expected in September 2015).

Summary

Increasing efficiency, reducing CO_2 emission and fuel consumption are of the most important challenges in high temperature technologies. Higher efficiencies can be achieved by increasing the operating conditions (temperature and pressure). This has challenged materials science community to improve high temperature properties of the existing materials or pursue novel materials for higher temperatures. For more than 60 years this goal was achieved by enhancing the high temperature properties of Ni-base superalloys. Modification of the composition with more than 10 micro-macro alloying elements and engineering of the microstructure with γ -γ' phase system has significantly increased its mechanical properties and environmental resistance till up to 1150°C. However, due to the softening of Ni above 1150°C there is no more scope to increase the service temperature of such alloys[1, 2] and demands raised for new materials replacing Ni-base superalloys.

Chromium and its alloys are considered as potential candidate for high temperature applications because of its high melting point (1900°C), low density (7.15 g/cm3) (Ni=8.90 g/cm3) and high-temperature oxidation resistance. These advantages are negated by low ductility at room temperatures (a typical feature in all bcc metals), Nitrogen embrittlement at high temperature due to severe nitridation, and low oxidation resistance at ultra-high temperatures (>1000°C) due to volatilization[7-9]. Researchers have been working on enhancing the mechanical and high temperature performance of Cr-based alloys by micro-macro alloying with binary-ternary or quaternary elements such as Al, Ag, Si, Mo, Ta, W, Ru, Ce, and Nb. As a result of alloying, some of the drawbacks are improved. Some of the alloying elements form a two phase system with chromium composed of a toughening Cr solid solution phase along with an intermetallic hardening phase which is formed via solidification and thus are called in-situ composites. Cr_{ss}-Cr_2X alloys (X= Nb, Hf,Ta, Zr) form a eutectic microstructure containing laves phase Cr_2X particles or lamellae dispersed in a solid solution phase (Cr_{ss}). Cr_{ss}-Cr_3Si system forms a lamellar eutectic structure consisting of Cr_{ss} and Cr_3Si A15 phase. In this system, the A15 intermetallic phase is a source of high temperature strength and oxidation resistance and Cr_{ss} is a potential source of ductility.

In this work, at the first stage, we focused on understanding the oxidation behavior and the evolution of substrate alloy microstructure of alloys in the Cr-Si system. Nitridation was for the first time systematically studied in this system. It was found that the A15 silicide show superior oxidation resistance and high temperature stability in O_2-N_2 atmosphere (air). In two phase Cr-Cr3Si system the silicide phase forms under the oxide scale and protect the substrate microstructure against nitridation.

At the second stage, the Cr-Si-Ge ternary system was characterized for the first time at high chromium end. The ternary phase diagram was developed. And the effect of Ge-Si substitution on the crystallography (lattice parameter), microstructural evolution and oxidation-nitridation behavior of the Cr-Si-Ge was determined. It was found that all alloys with 84 at% Cr lay in two phase Cr-Cr_3(Ge,Si) and any proportion of Ge/Si is miscible in both Cr_{ss} and A15 phase. The fact that Ge promotes the formation of A15 in Cr-Ge system was used to modify the Cr-Cr3Si structure to improve its high temperature oxidation-nitridation resistance. It was found that the optimum amount of 2 at% Ge is highly beneficial against nitridation-oxidation of the Cr-Cr_3(Si,Ge). Ge-alloying reduced the dissolution rate of Cr_{ss} phase (which is the preferred Cr supply for scaling process) and accordingly, the oxidation kinetics was controlled. In addition, Ge promoted the A15 phase and disconnected the fine network of Cr_{ss} phase (sensitive to nitridation). The microstructure of Ge-alloyed Cr-Cr_3(Si, Ge) system was protected against nitridation for up to 1000 hours during oxidation at 1200°C in air. The strategy developed in this work solved one of the biggest obstacles to employ Cr alloys and facilitated further developments of such alloys for high temperature structural applications.

References

1. Y. Gu, H. Harada and Y. Ro, *JOM Journal of the Minerals, Metals and Materials Society*, **56**, 28 (2004).
2. H. Bei, G. M. Pharr and E. P. George, *Journal of Materials Science*, **39**, 3975 (2004).
3. K. Yoshimi, S. Nakatani, N. Nomura and S. Hanada, *Intermetallics*, **11**, 787 (2003).
4. B. P. Bewlay, J. A. Sutliff, M. R. Jackson and K. M. Chang, *Materials and Manufacturing Processes*, **9**, 89 (1994).
5. B. P. Bewlay, M. R. Jackson, P. R. Subramanian and J. C. Zhao, *Metallurgical and Materials Transactions A*, **34**, 2043 (2003).
6. B. V. Cockeram and R. A. Rapp, *Materials Science and Engineering: A*, **192-193, Part 2**, 980 (1995).
7. Y. F. Gu, H. Harada and Y. Ro, *JOM*, **56**, 28 (2004).
8. L. Royer, X. Ledoux, S. Mathieu and P. Steinmetz, *Oxid Met*, **74**, 79 (2010).
9. D.J. Young, High temperature oxidation and corrosion of metals, 1 ed., Access Online via Elsevier, 2008.
10. A. Bhowmik, H. T. Pang, I. M. Edmonds, C. M. F. Rae and H. J. Stone, *Intermetallics*, **32**, 373 (2013).
11. S. V. Raj, J. Daniel Whittenberger, B. Zeumer and G. Sauthoff, *Intermetallics*, **7**, 743 (1999).
12. M. Takeyama and C. T. Liu, *Materials Science and Engineering: A*, **132**, 61 (1991).
13. H. Bei, E. P. George and G. M. Pharr, *Intermetallics*, **11**, 283 (2003).
14. M. P. Brady, P. F. Tortorelli, E. A. Payzant and L. R. Walker, *Oxidation of Metals*, **61**, 379 (2004).
15. M. P. Brady, C. T. Liu, J. H. Zhu, P. F. Tortorelli and L. R. Walker, *Scripta Materialia*, **52**, 815 (2005).
16. Dogan.Ö.N., *Oxidation of Metals*, **69**, 233 (2008).
17. Y. Gu, Y. Ro, T. Kobayashi and H. Harada, *Metallurgical and Materials Transactions A*, **36**, 577 (2005).
18. Y. Gu, Y. Ro and H. Harada, *Metallurgical and Materials Transactions A*, **35**, 3329 (2004).
19. A. Gali, H. Bei and E. P. George, *Acta Materialia*, **57**, 3823 (2009).
20. M. P. Brady, C. T. Liu, J. H. Zhu, P. F. Tortorelli and L. R. Walker, *Scripta Materialia*, **52**, 815 (2005).
21. T. A. Cruse and J. W. Newkirk, *Materials Science and Engineering: A*, **239–240**, 410 (1997).
22. J. A. Sago and J. W. Newkirk, *Intermetallic Matrix Composites*, **194**, 183 (1990).
23. S. V. Raj, *Materials Science and Engineering: A*, **201**, 229 (1995).
24. J. Ang, V. A. Vorontsov, C. L. Hayward, G. Balakrishnan, H. J. Stone, C. M. F. Rae, Cambridge Univ Press, 2011.
25. T. Kitashima, K. S. Suresh and Y. Yamabe-Mitarai, *Materials Science and Engineering: A*, (2014).
26. W. Wang, B. Yuan and C. Zhou, *Corrosion Science*, **80**, 164 (2014).
27. B. V. Cockeram and R. A. Rapp, *Oxidation of Metals*, **45**, 427 (1996).
28. Z. Li and P. Tsakiropoulos, *Intermetallics*, **19**, 1291 (2011).
29. Z. Li and P. Tsakiropoulos, *Journal of Alloys and Compounds*, **550**, 553 (2013).
30. A. Soleimani-Dorcheh, W. Donner and M. C. Galetz, *Materials and Corrosion*, DOI: 10.1002/maco.201307423 (2014).
31. J. B. Nelson and, *Proceedings of the Physical Society*, **57**, 160 (1945).
32. A. Soleimani-Dorcheh and M. C. Galetz, *Oxid Met*, 1 (2015).
33. M. H. Sluiter, *Physical Review B*, **80**, 220102 (2009).
34. S. Prasad and A. Paul, *Journal of Phase Equilibria and Diffusion*, **32**, 212 (2011).
35. N. V. Starostina, S. V. Prikhodko, A. J. Ardell and S. Prasad, *Materials Science and Engineering: A*, **397**, 264 (2005).
36. A. Soleimani-Dorcheh and M. C. Galetz, *Metall and Mat Trans A*, **45**, 1639 (2014).